

## **VOIDS IN FIBER REINFORCED THERMOSETTING POLYMERS: FORMATION, STRUCTURE AND MECHANICAL BEHAVIOUR**

Ivan V. Sergeichev<sup>1</sup>, Eduard S. Batyrshin<sup>2</sup>, Almir I. Mullayanov<sup>2</sup>, Svyatoslav S. Chugunov<sup>1</sup>,  
Sergey G. Abaimov<sup>1</sup>, Iskander Sh. Akhatov<sup>1</sup>

<sup>1</sup> The Center for Design, Manufacturing and Materials, Skolkovo Institute of Science and Technology,  
Nobel Str. 3, Moscow, 143026, Russia, [i.sergeichev@skoltech.ru](mailto:i.sergeichev@skoltech.ru), <http://www.skoltech.ru>

<sup>2</sup> The Center for Micro- and Nanoscale Dynamics of Dispersed Systems  
Bashkir State University, Zaki Validi Str. 32, Ufa 450076, Russia, [batyrshine@mail.ru](mailto:batyrshine@mail.ru),  
<http://www.bashedu.ru>

**Keywords:** Glass-fiber reinforcement, polymer matrix composite, liquid composite molding, voids,  
computed micro-tomography, microscopy

### **ABSTRACT**

Modern technological operations require production of void-free laminates with the optimal degree of resin cure, using fiber-reinforced composite materials with thermosetting matrix as a basis. Formation of voids in composite laminate is a complex physical process, which depends on an interaction of heat transfer, resin flow, pre-form compaction and cure process. When composites were first introduced, formation of large voids was inevitable, since parameters of manufacturing process (i.e., temperature/pressure-time profiles) were selected via empirical methods. To disadvantage of such an approach, the parameters were restricted to a small range of process variables; they could not be generalized for different materials and geometries; finally, the method was expensive and time consuming. The shortcomings of empirical approach could be eliminated with the use of validated analytical and numerical models of composite material, which allow optimization of the process variables.

The present work is focused on experimental research of void formation during impregnation of unidirectional glass-fiber reinforcement with thermosetting polymer resin. A number of samples featuring various degree of porosity and different void structure were prepared with liquid composite molding (LCM) technique. The designed mold allows an impregnation of the dry unidirectional preform under pressure gradient, created by pressure difference at inlet and outlet of the mold. Composite samples were fabricated at a variety of pressure conditions at inlet and outlet of the mold, replicating injection and infusion processes. Void distribution and volume fraction of voids in the sample volume were studied using optical microscopy and computed micro-tomography techniques.

### **1 INTRODUCTION**

Porosity is one of the most critical technological defects of fiber-reinforced composite materials, regardless of the reinforcement type and methods of production. In the general case, the porosity is determined as the volume concentration of interfacial voids arranged in a matrix between fiber layers and/or inside bundles of fibers, and distributed throughout the thickness of laminated polymer composites. The formation of macro - and micro-porosity structure in fiber-reinforced composite materials owes to hydrodynamic instability of the flow of liquid resin between the fibers and the entrapment of air bubbles and volatile substances, which is determined by the content of gaseous fractions and plasticizing additives in the original resin. In addition, a possible void formation mechanism at micro-level could be attributed to peculiarities of chemical reactions of polymerization when thermosetting resins are used, or to a crystallization process, in the case of thermoplastic resins. These factors depend on local velocities of liquid resin flow in a preform, moisture content and gas content in the resin, temperature and pressure values during resin cure, etc.

Development and introduction of novel technologies for manufacturing of composite materials generally requires large amount of expensive technological experiments to obtain parameters, governing the production process. They ensure that critical material properties match the expectations in the final product. However, precise control of product's properties at different volume locations is not possible at

all production stages. Based on these factors, determining, in particular, formation of porosity network in fiber-reinforced composite materials, it becomes apparent that under industrial production settings there should be special measures taken to ensure sustainable production of composite material with the required physical and mechanical properties.

In modern industrial applications, manufacturing quality of composites is often determined by bulk measurement of porosity volume and verified by microscopic examination of selected specimen sections. While volumetric inspection methods provide total porosity content in the specimen, they do not correctly assess voids distribution and clustering in sample's volume, which are critical factors for structural performance of composites [1,2]. Microscopic examination allows high-quality measurement of voids in specific cut sections, but inadequate representation of voids in the selected sections may lead to wrong conclusions.

Mechanical properties of composites are dramatically influenced by volume fraction and distribution of voids, this is especially true for interlaminar shear strength [3], modulus of elasticity and compressive strength [4], bending resistance [5], and interlaminar fracture toughness [6]. As an example, for layered fiber-reinforced thermoplasts, the interlaminar shear strength is reduced by more than 30% with void volume fraction increasing from 0.5% to 5.6% [7].

Additional type of engineering problems, related to morphology of voids, is concerned with composite strength under fatigue condition. A mechanism of fracture development under cyclic loading is not determined by void volume fraction alone; it rather depends on the presence of major defects in critical areas of the sample [8]. Therefore, in-depth analysis of void network structure and morphology is of great interest for practical applications. For instance, an employment of computed microtomography technique allows determining location of large voids, void clusters, and nucleation spots for fatigue-induced fractures [9]. In [9], a clear correlation between voids volume fraction and fatigue resistance of composite was observed, when the former increased from 0.8% to 3%. At the same time, bulk porosity could not be correlated with density of fracture network and degradation of laminate stiffness under cyclic tension [10]. Importance of void morphology study in connection to interlaminar fracture toughness  $G_{IC}$  under cyclic loading was also outlined [6].

Porosity formation mechanisms are attributed to both, the impregnation and the curing stage of composite manufacturing process. During the impregnation stage, a non-uniform propagation of resin front leads to formation of voids. This process could be invoked due to non-optimal design of the shape and arrangement of supply and vacuuming ports, to complex placement of reinforcement material, as well as to flow instabilities at different scales, caused by competition between capillary effects and viscous forces. For example, individual voids could be attributed to the areas of higher and lower permeability (edges, bends and special layers) [11], or to the zones where irregularities in fiber placement favour either capillary or viscous processes inside of bundles (inter-tow) and between the bundles (intra-tow) of fibers [12]. During the curing stage, porosity may form in the result of evaporation of volatile resin components into micro-bubbles [13].

## 2 EXPERIMENTAL PROCEDURES

### 2.1 Materials selection

Sample fabrication procedure was based on the use of commercially available Epolam 2040 epoxy resin and Epolam 2042 hardener (Axson Technologies, France) with mixing ratio 100:31, by weight. The initial viscosity of a mixture was 280 mPa·s and the gel time was 100 min at 25°C. Due to the low viscosity, the manufacturer's suggested manufacturing application for this epoxy resin is liquid resin infusion molding. The reinforcement material consisted of a direct E-CR glass fiber roving PS 2100 (Owens Corning, USA) with linear density of 2400 tex. Each roving thread consisted of about 2000 filament; average diameter of individual filaments was 24 μm.

### 2.2 Experimental setup

The experimental setup utilized for samples manufacturing (Fig.1) allows injection of epoxy resin into the mold using compressed air pressure applied to the inlet of the system or resin infusion under the

action of a vacuum applied to the outlet of the system. The transparent mold was made of acrylic glass. It contains a rectangular cavity with dimensions of  $6.3 \times 16 \times 140$  mm, where glass-fiber roving is impregnated with the resin to form composite plates. The different parts of the setup were interconnected with 4 mm polyethylene tubes.

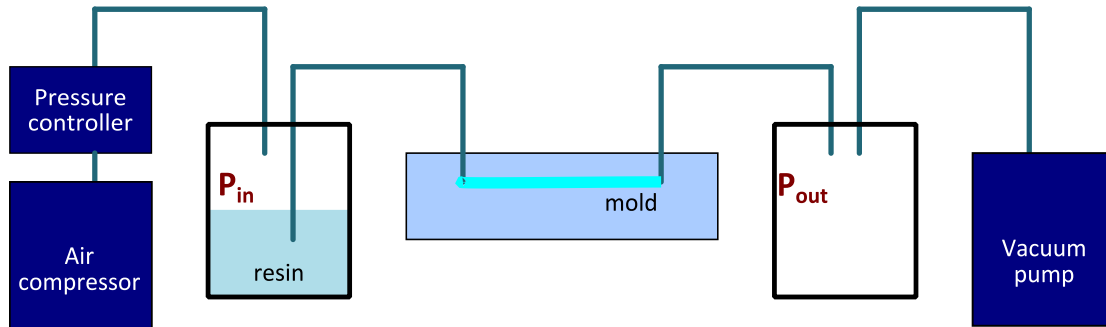


Figure 1: Schematic representation of the experimental setup designed for manufacturing of fiber-reinforced composite samples via injection or infusion techniques

### 2.3 Samples manufacturing

Fiber rovings were placed into the mold cavity in the longitudinal direction, attention was paid to ensure unidirectional reinforcement. The total amount of threads was 70, which corresponds to 63% volume fraction of fibers. The epoxy resin and the hardener were mixed with a rotational mixer at 1000 rpm for 15 minutes, following by degassing in a vacuum chamber. All composite samples, presented in this work, were manufactured by air pressure driven resin injection. During the injection stage, the inlet pressure  $P_{in}$  and the outlet pressure  $P_{out}$  were kept constant, so the corresponding pressure difference was  $\Delta P = P_{in} - P_{out}$ . The inlet and outlet pressure values are given in Table 1 for the six manufactured groups of samples. Each group consisted of 5-6 samples. The impregnation process was stopped at the moment, when resin front reached the outlet. The obtained composite plates were cured for 24 hours at room temperature, following by 16 hours of curing in an oven at  $70^{\circ}\text{C}$ , as per recommendation of the resin manufacturer. Image of a cured composite plate is shown in the Fig.2.

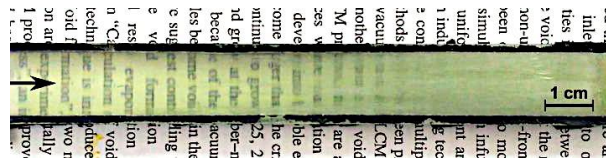


Figure 2: A typical composite plate produced by resin infusion method. Resin inflow direction is indicated by the arrow. A gradient in plate's transparency indicates variation of porosity along the length of the plate.

Sample group	Inlet pressure, MPa	Outlet pressure, MPa
1	0	-0.095
2	0.02	-0.08
3	0.04	-0.06
4	0.06	-0.04
5	0.08	-0.02
6	0.1	0

Table 1: Inlet and outlet pressure values applied to the mold, pressure values are shown relative to standard conditions.

## 2.4 Microscopy

A typical cured composite plate is presented in Fig.2. A noticeable transparency gradient is present in the sample. The gradient is formed due to the variation of porosity content along the length of the sample. One of the widely used and precise characterization methods for void content estimation is based on the use of optical microscopy and image analysis techniques [14]. To assess the variation of voids, the composite plate was sectioned into 10-mm sub-samples along the plate length, using a water-cooled diamond saw. Each sub-sample was prepared for optical microscopy by successive polishing of the cut surface with 240-600-1200-2500 grit size grinding paper. The final polish was made with a diamond paste with the size of abrasive particles 2-3  $\mu\text{m}$ . After every polishing operation, sub-samples were cleaned in an ultrasonic bath.

For estimation of overall void content and their spatial distribution over the cut surface, sub-samples of the composite sample were studied with Olympus IX-71 microscope and Lumenera Infinity-2 camera with spatial resolution of 1  $\mu\text{m}/\text{pixel}$ .

## 2.4 Micro-Tomography

Study of composite 3D structure was carried with micro-tomography analysis, employing GE v|tome|x m300 (General Electric, USA) microtomograph with 1  $\mu\text{m}/\text{voxel}$  resolution, at 100 kV, 100 mA. Because of the physical restrictions of X-Ray tomography, only a  $5.5 \times 5.5 \times 4.3$  mm portion of the original sample could be imaged with such a high resolution. The numerically reconstructed 3D grayscale image contained X-Ray attenuation values at each voxel, which could be interpreted as density of the material occupying such voxels. The 3D image was processed with edge-preserving smoothing and sharpening filters. Three material phases – matrix, fibers, and voids - were segmented in the volume of the image, using histogram values for evaluation of threshold levels.

The segmented models were used for qualitative analysis of composite structure. The quantitative analysis requires handling of multiple uncertainties at interfaces between different material phases – this is the subject of future research.

## 3 RESULTS

### 3.1 Microscopy

Fig.3 illustrates typical images of sample cross sections close to the inlet, to the outlet and to the center of the mold. Note that approximately 1/30 of the entire images of cross sections are shown in the Fig.3. Matrix, fiber, and void phases can be easily distinguished in images - voids appear as dark spots. The cross-section images were binarized using thresholds obtained from image histograms. Void content was estimated as a ratio of dark area to the whole area of cross section. Results obtained for all sub-samples are shown in the Fig.4. The evolution of void content along the sample (Fig. 4) indicates growth of porosity when distance from the inlet increases.

The error in porosity estimations is mainly due to the uncertainty in the choice of the threshold values for image binarization. It should be noted that only the transverse dimensions of voids were determined. Obtained data were used to estimate volumetric void content of the samples. The lack of data on the voids size in the third dimension leads to an additional error, but if the voids have a shape close to either spherical or cylindrical, such an error is small.

Voids in the inner structure of composites are created because of mechanical air entrapment during the resin impregnation stage. Entrapped air bubbles flow with resin, but bubble velocity differs from velocity of resin flow. Mobility of bubbles results in a low voidage close to mold inlet. Generation of bubbles and their transport determine the distribution of voids along the sample. The result shown in Fig.4 is qualitatively consistent with the prediction of multiphase flow models [15].

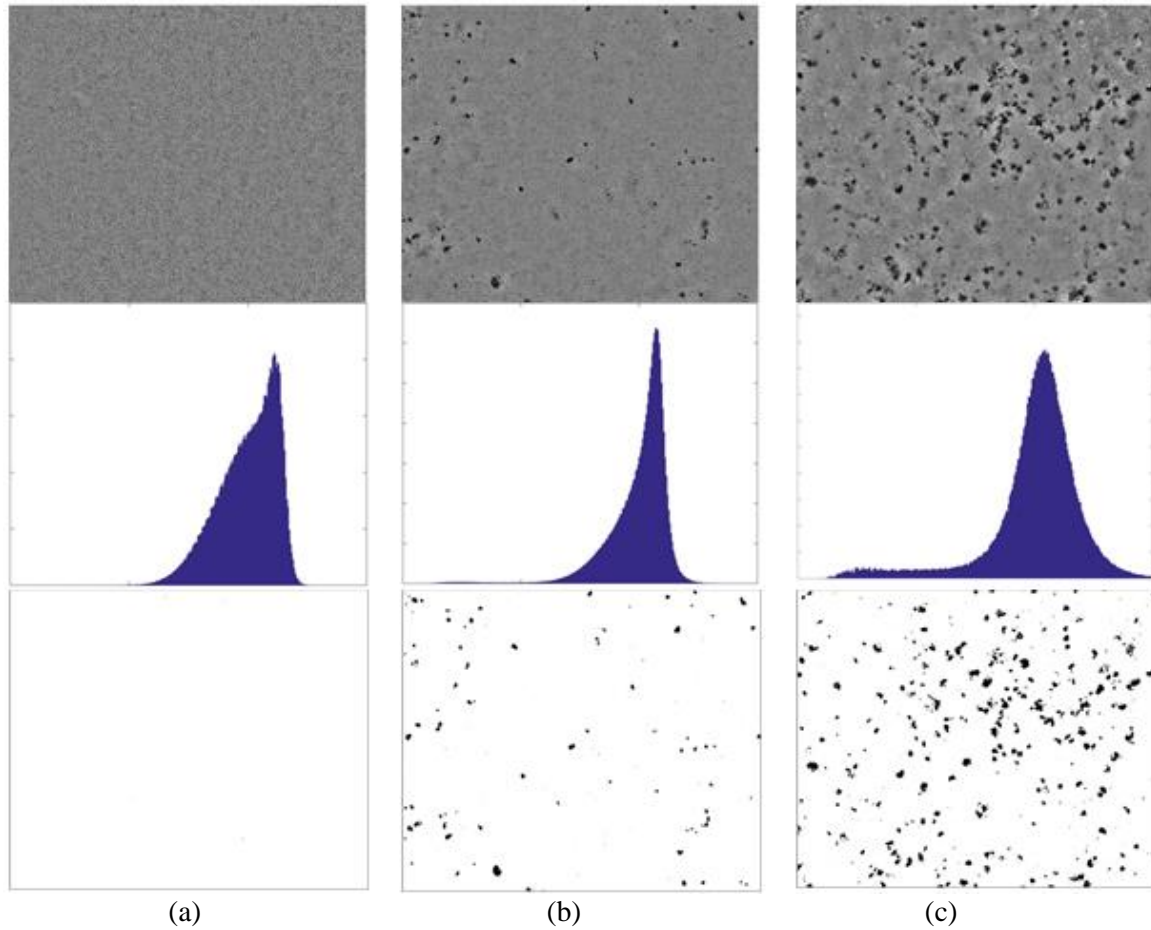


Figure 3: Microscopy images of samples' cross section (top row) and corresponding intensity histograms (bottom row). The shown are void distribution (a) at the inlet, (b) at the center, and (c) at the outlet of the mold.

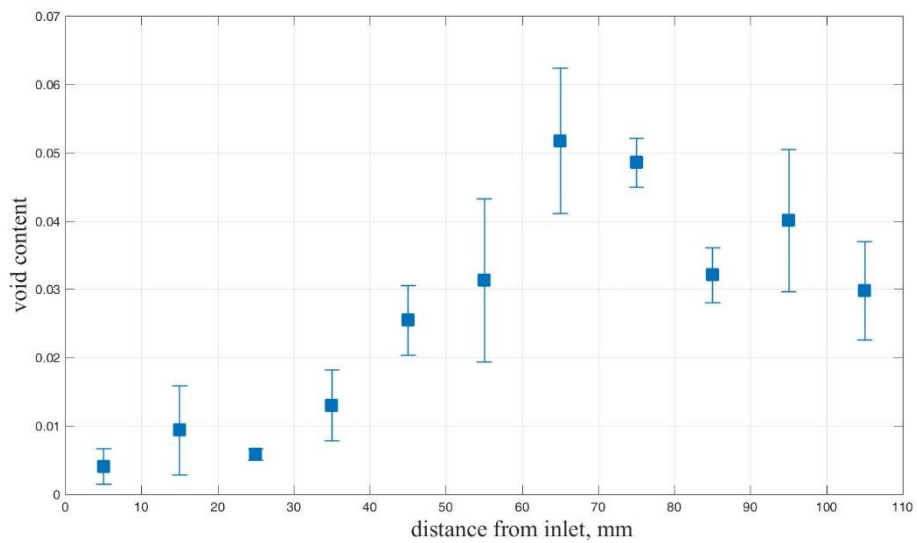


Figure 4: Void content evolution along the composite sample.

### 3.2 Micro-Tomography

Micro-tomography technique provides a good insight into composite internal structure. For the sample of glass-fiber reinforced polymer-matrix composite, there was a  $5.5 \times 5.5 \times 4.3$  mm volume region imaged with  $2 \mu\text{m}/\text{voxel}$  resolution, out of the  $65 \times 6.5 \times 6.5$  total volume of the sample. A part of the 3D structural model of the composite, prepared with image processing tools is shown in Fig 5. There were 3 phases segmented: the matrix, the fibers, and the pores. For the fibers, the overall characteristics were considered, such as location of individual fibers, their shape, curvature, alignment with other fibers.

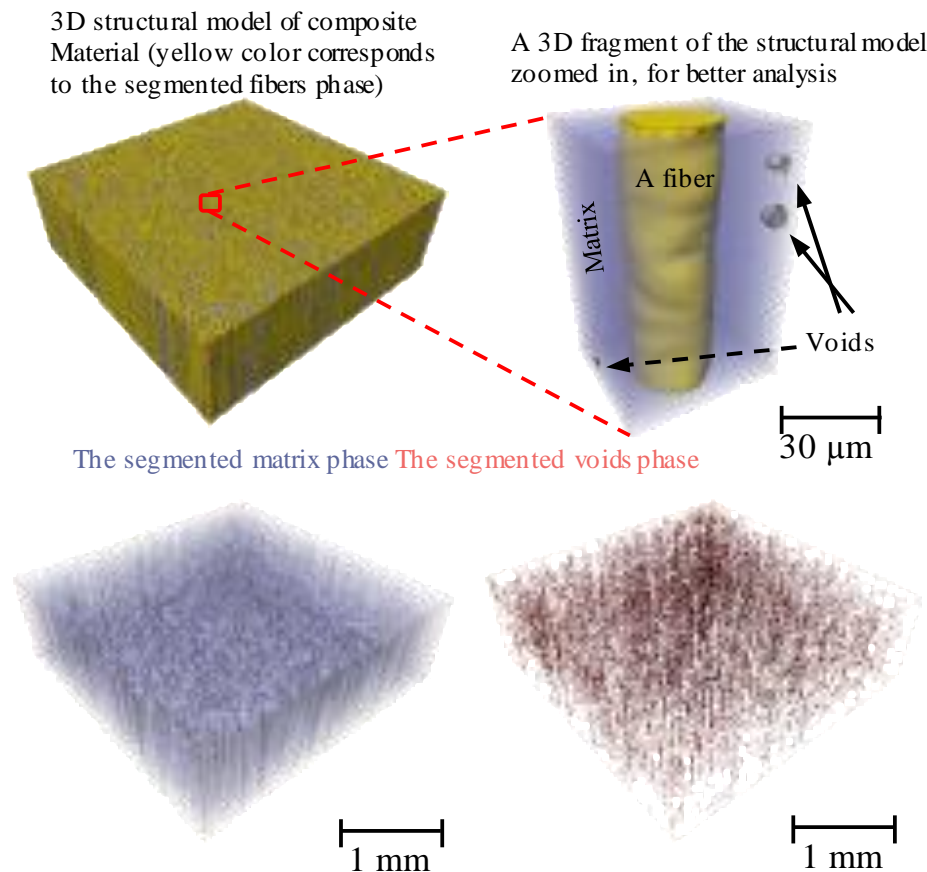


Figure 5: A structural 3D model of the manufactured sample.

In the Fig.5, a structural 3D model of the manufactured sample (top left) is segmented into the matrix phase (bottom left), the voids phase (bottom right) and the fibers phase (shown together with matrix and voids at the top left). Every part of the model is presented at  $1 \mu\text{m}/\text{voxel}$  resolution, which allows studying small details of voids morphology and topology in relation to the matrix and fibers (top right).

The fiber phase was separated into individual fibers (Fig 6). Voids, situated near individual fibers (Fig 5, top right) were analyzed in terms of their shape, orientation, roughness, connection to the fiber phase. The shape of the voids and their position in relation to matrix and fibers could be used as an indicator of the physical process, that influences void formation. Small voids could be separated from large voids; void clusters could be identified as the next step of the analysis of composite structure.

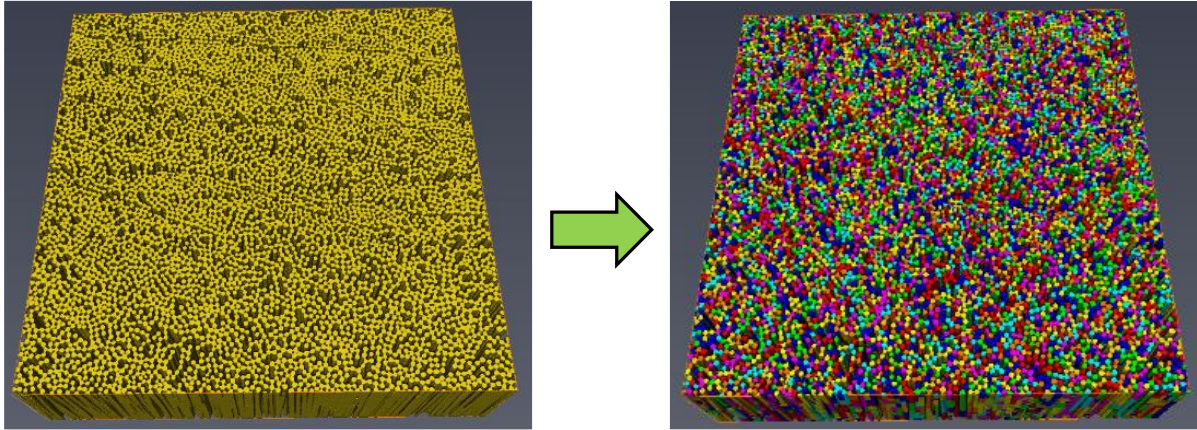


Figure 6: Segmented fibers (left) separated from each other (right) to prepare the structural model for quantitative analysis

The data collected in this work are to be used for formulation of a 3D numerical model, suitable for direct numerical simulations of epoxy resin impregnation process, resin curing process, and mechanical behavior of the cured composite material. The geometry, acquired with micro-tomography technique, would serve as the input into finite element numerical models and micromechanical analytical models for further analysis in attempt to find correlations between porosity characteristics and physical-mechanical properties of the composite.

#### 4 CONCLUSIONS

A method for manufacturing fiber-glass reinforced composite samples with control over lengthwise porosity distribution was developed, based on liquid composite molding technique. The method allows manufacturing samples with variety of void content, by adjusting inlet and outlet pressure of the mold. Using this method, a group of six samples was manufactured for microstructural studies.

Voids distribution in the volume of unidirectional fiber reinforced composite samples was studied using optical microscopy and computed micro-tomography techniques. A gradient in concentration of voids along the sample length was observed, with the number of voids increasing towards the outlet. The obtained results are qualitatively consistent with the prediction of multiphase flow models [15].

Analysis of voids properties, using multiple examination techniques allows detailed exploration of local effects in the sample volume and provides input data for formulation of a 3D numerical model, suitable for direct numerical simulations of epoxy resin impregnation process, resin curing process, and mechanical behavior of reinforced composite materials. Besides the injection/infusion process, the demonstrated technique could be applied to other manufacturing methods and composite types.

Further experiments to study the effect of inlet/outlet pressure conditions during the preform impregnation on the distribution of voids in the bulk of the sample and void morphology will provide more detail on the mechanisms of void formation.

#### ACKNOWLEDGEMENTS

The presented project has partly funded in the framework of the Master Research Agreement between the Center for Design, Manufacturing and Materials of Skolkovo Institute of Science and Technology and the Center for Micro- and Nanoscale Dynamics of Dispersed Systems of Bashkir State University (#1646-MRA).

#### REFERENCES

- [1] Lambert J., Chambers A.R., Sinclair I., Spearing S.M. 3D damage characterisation and the role of voids in the fatigue of wind turbine blade materials. *Composites Science and Technology*, **72**, 2012, pp. 337–343 (doi:[10.1016/j.compscitech.2011.11.023](https://doi.org/10.1016/j.compscitech.2011.11.023)).

- [2] Nikishkov Y., Seon G., Makeev A. Structural analysis of composites with porosity defects based on X-ray Computed Tomography, *Journal of Composite Materials*, **48**, 2014, pp. 2131–2144. (doi:[10.1177/0021998313494917](https://doi.org/10.1177/0021998313494917)).
- [3] Costa M.L., Rezende M. C., Frascino S.M. The influence of porosity on the interlaminar shear strength of carbon/epoxy and carbon/bismaleimide fabric laminates, *Composites Science and Technology*, **61**, 2001, pp. 2101–2108
- [4] Kosmann N., Karsten J.M., Schuett M., Schulte K., Fiedler B. Determining the effect of voids in GFRP on the damage behaviour under compression loading using acoustic emission, *Composites: Part B*, **70**, 2015, pp. 184–188.
- [5] Hagstrand P.O., Bonjour F., Manson J.A.E. The influence of void content on the structural flexural performance of unidirectional glass fibre reinforced polypropylene composites, *Composites: Part A*, **36**, 2005, pp.705-714.
- [6] Hakim I.A., Donaldson S.L., Meyendorf N. G., Browning Ch. E. Porosity effects on Interlaminar fracture behavior in carbon fiber-reinforced polymer composites, *Materials Sciences and Applications*, **8**, 2017, pp. 170-187 (doi:[10.4236/msa.2017.82011](https://doi.org/10.4236/msa.2017.82011)).
- [7] Bhat M.R., Binoy M.P., Surya N.M., Murthy C.R.L. and Engelbart R.W. Non-destructive evaluation of porosity and its effect on mechanical properties of carbon fiber reinforced polymer composite materials. Review of progress in quantitative nondestructive evaluation, *AIP Conferences Proceedings*, **1430**, 2012, pp. 1080-1087.
- [8] Chambers A.R., Earl J.S., Squires C.A., Suhot M.A. The effect of voids on the flexural fatigue performance of unidirectional carbon fibre composites developed for wind turbine applications, *International Journal of Fatigue*, **28**, 2006, pp. 1389–98.
- [9] Maragoni L., Carraro P.A., Quaresimin M. Effect of voids on the crack formation in a [45/-45/0]<sub>s</sub> laminate under cyclic axial tension, *Composites: Part A*, **87**, 2016, pp.116–127 (doi:[10.1016/j.compositesa.2016.02.018](https://doi.org/10.1016/j.compositesa.2016.02.018)).
- [10] Maragoni L., Carraro P. A., Peron M., Quaresimin M. Fatigue behaviour of glass/epoxy laminates in the presence of voids, *International Journal of Fatigue*, **95**, 2017, pp.18–28 (doi:[10.1016/j.ijfatigue.2016.10.004](https://doi.org/10.1016/j.ijfatigue.2016.10.004)).
- [11] Sas H.S., Šimáček P., Advani S.G. A methodology to reduce variability during vacuum infusion with optimized design of distribution media, *Composites: Part A*, **78**, 2015, pp.223–233.
- [12] Michaud V. A., Review of Non-saturated Resin Flow in Liquid Composite Moulding processes, *Transport in Porous Media*, **3**, 2016, pp. 581–601.
- [13] Pupin C., Ross A., Dubois Ch., Rietsch J.Ch., Vernet N., and Ruiz E. Formation and suppression of volatile-induced porosities in an RTM epoxy resin, *Composites: Part A*, **94**, 2017, pp.146–157.
- [14] Hayes B. S., Gammon L. M., Optical microscopy of fiber-reinforced composites, *ASM International*, 2010, ISBN 9781615030446.
- [15] Gascón L., García J. A., LeBel F. et al. A two-phase flow model to simulate mold filling and saturation in resin transfer molding, *International Journal of Material Forming*, 2016, **9**, pp. 229–239.